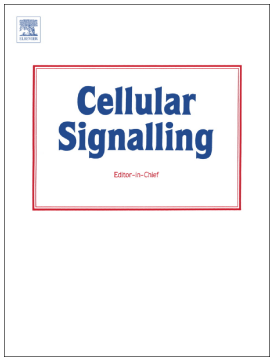

Rac1 plays a role in CXCL12 but not CCL3-induced chemotaxis and Rac1 GEF inhibitor NSC23766 has off target effects on CXCR4

Shirley C. Mills, Lesley Howell, Andrew Beekman, Leanne Stokes, Anja Mueller

PII: S0898-6568(17)30274-7
DOI: doi:10.1016/j.cellsig.2017.10.006
Reference: CLS 9014

To appear in: *Cellular Signalling*

Received date: 30 May 2017
Revised date: 11 October 2017
Accepted date: 13 October 2017

Please cite this article as: Shirley C. Mills, Lesley Howell, Andrew Beekman, Leanne Stokes, Anja Mueller , Rac1 plays a role in CXCL12 but not CCL3-induced chemotaxis and Rac1 GEF inhibitor NSC23766 has off target effects on CXCR4. The address for the corresponding author was captured as affiliation for all authors. Please check if appropriate. Cls(2017), doi:10.1016/j.cellsig.2017.10.006

Rac1 plays a role in CXCL12 but not CCL3-induced chemotaxis and Rac1 GEF inhibitor NSC23766 has off target effects on CXCR4

Shirley C Mills[1], Lesley Howell[1,2], Andrew Beekman[1], Leanne Stokes[1] and Anja Mueller[1]

1) School of Pharmacy, University of East Anglia, Norwich Research Park, Norwich NR4 7TJ, UK

2) Current address: School of Biological and Chemical Sciences, Queen Mary, Mile End Road, London, E1 4NS

Running title: Rac1 activation is important for CXCR4 chemotaxis

Corresponding author: - Anja Mueller, School of Pharmacy, University of East Anglia, Norwich Research Park, Norwich NR4 7TJ, UK

Phone: 44 1603 593138

Email: anja.mueller@uea.ac.uk

Abstract

Cell migration towards a chemotactic stimulus relies on the re-arrangement of the cytoskeleton, which is triggered by activation of small G proteins RhoA, Rac1 and Cdc42, and leads to formation of lamellopodia and actin polymerisation amongst other effects. Here we show that Rac1 is important for CXCR4 induced chemotaxis but not for CCR1/CCR5 induced chemotaxis. For CXCL12-induced migration via CXCR4, breast cancer MCF-7 cells are reliant on Rac1, similarly to THP-1 monocytes and Jurkat T-cells. For CCL3-induced migration via CCR1 and/or CCR5, Rac1 signalling does not regulate cell migration in either suspension or adherent cells. We have confirmed the involvement of Rac1 with the use of a specific Rac1 blocking peptide. We also used a Rac1 inhibitor EHT 1864 and a Rac1-GEF inhibitor NSC23766 to probe the importance of Rac1 in chemotaxis. Both inhibitors did not block CCL3-induced chemotaxis, but they were able to block CXCL12-induced chemotaxis. This confirms that Rac1 activation is not essential for CCL3-induced migration, however NSC23766 might have secondary effects on CXCR4. This small molecule exhibits agonistic features in internalisation and cAMP assays, whereas it acts as an antagonist for CXCR4 in migration and calcium release assays. Our findings strongly suggest that Rac1 activation is not necessary for CCL3 signalling, and reveal that NSC23766 could be a novel CXCR4 receptor ligand.

Keywords: chemokine receptor, chemotaxis, antagonist, Rac1, ligand bias

Abbreviations

AUC – Area under Curve

EDTA - Ethylenediaminetetraacetic acid

FCS - Foetal calf serum

FSC – Forward scatter

GPCR – G protein-coupled receptor

PBS - Phosphate buffered saline

SEM – Standard Error of Means

SSC –Side scatter

1. Introduction

Chemokines are small proteins produced by cells that can trigger cellular migration activated by G protein-coupled receptors (GPCRs), called chemokine receptors [1]. Particularly in cancer, it has been shown that these chemokine receptors play a critical role in inducing the migration of cancer cells to different parts of the body [2, 3]. Several chemokine receptors are highly expressed on cancer cells, including CXCR4, CCR5 and CCR1 [4-10]. Chemokine receptors may initiate signalling through binding a ligand, a specific chemokine or a chemical. CXCL12 binds to and activates the CXCR4 and CXCR7 receptors, but it is thought that only CXCR4 activation leads to chemotaxis of cells [11]. CCL3 is a ligand for both CCR5 and CCR1; it can activate both receptors and lead to a migratory response in cells [12]. Several other ligands can also bind to either CCR1 or CCR5 or both [12, 13]. In general, chemokine receptor activation leads to an activation of heterotrimeric G proteins and phosphorylation of the receptors via GRKs (G protein-coupled receptor kinases) or PKC (protein kinase c). This leads to the binding of arrestins to the phosphorylated form of the receptor and causes receptor internalisation [12, 14]. Traditionally it is thought that βγ-subunits of the G proteins induce migration via activation of PI3K [15], however we have recently shown that this seems not to be the case for CCL3-induced chemotaxis in THP-1 cells [16] whereas PI3K is important for CXCL12-induced migration [5]. Both CXCL12 and CCL3-induced migration relies on the activation of Src, whereas the involvement of PKC seems to be cell type dependant [5].

Re-arrangement of the actin cytoskeleton is of major importance for chemotaxis, and the small G proteins of the rho family (rho, rac and cdc42) play

important roles in this [17]. Actin filament reorganization is a dynamic process that requires both actin polymerizing and depolymerizing factors [18]. Specifically, Cdc42 and Rac1 regulate filopodia and lamellopodia formation, respectively, while RhoA regulates stress fibres and focal adhesion [19]. It has been well documented that activation of chemokine receptors leads to the occurrence of actin stress fibres and membrane ruffling [20-22]. It has also been shown that the blocking of RhoA or ROCK (rho-activated kinase) prevents migration of cells [16]. However, it is not known how chemokines and their receptors regulate the actin cytoskeleton leading to metastasis of cancer cells [23, 24]. In leukocytes, chemokine receptors control activation of a small G protein, Rac1, which induces growth of actin filaments. Recent studies have shown that Rac1 is associated with CXCL12-induced chemotaxis in breast cancer cells [24], as well as modulating cell invasion and tumour metastasis in human oesophageal cancer [25]. Direct association with Rac1 also seems to affect the conformation of CXCR4 [26] and therefore might affect chemokine binding to the receptor and activation of downstream signalling partners. In this study we examined the role of Rac1 in cell chemotaxis induced by two different chemokines, CCL3 and CXCL12 respectively, in different cellular backgrounds. These results highlight the importance of characterising cell signalling networks by single receptor, and not by families, as well as considering cellular background when analysing results.

2. Materials and Methods

2.1 Cells and materials

The leukemic cell line Jurkat and the monocytic cell line THP-1 were purchased from the ATCC (Teddington, UK) and both cell lines were grown as described [5]. The breast cancer cell line MCF-7 was obtained from the ATCC and grown in DMEM containing 10% FCS and 2 mM L-glutamine. The chemokine CXCL12 was obtained from Peprotech (London, UK); CCL3 has been described previously [16, 27]. NSC23766, AMD3100, and H89 were purchased from Abcam (Cambridge, UK). ATI2341 was from Tocris Biosciences (Bristol, UK), EHT1864 was purchased from Cambridge Biosciences (Cambridge, UK). The anti-CXCR4 (12G5) antibody was from R&D Systems (Abingdon, UK) and the corresponding FITC labelled anti-mouse secondary antibody was from Sigma (Poole, UK). Rac1 Pull-down Activation Assay Kit was obtained from Cytoskeleton Inc (Denver, USA), the CatchPoint cAMP Fluorescent Assay Kit was from Molecular Devices (Wokingham, UK). All other chemicals were from Fisher Scientific (Loughborough, UK).

2.2 Peptide synthesis:

Two 15mer peptides, active (VDGKPVNLGLWDTAG) (W56) and inactive (VDGKPVNLGLFDTAG) (F56) were synthesized on a Multisyntech Syro I automated peptide synthesiser using standard Nα-Fmoc-based solid-phase peptide synthesis. The synthesis was carried out on a NOVA PEG Rink amide polystyrene resin (substitution: 0.49 mmol/g) using methodology similar to that described by Malkinson [28], except that Fmoc de-protection was carried out with 40% piperidine (1 x 10 mins) and 20% piperidine (2 x 5 mins). The peptide was cleaved from the resin by shaking the resin beads in 5 mL TFA / H_2O / TIPS (95:2.5.2.5 %v/v) for 3 hrs. The solution was filtered and the resin beads washed with neat TFA and combined with the above solution. This was then evaporated under vacuum. The crude peptide was

precipitated with cold diethyl ether and then filtered. The peptides were purified using reverse phase chromatography on a Biotage Isolera Four (SNAP Cartridge KP-C18-HS 12g). Mobile phase A: 5% methanol in H_2O + 0.05% TFA. Mobile phase B: 5% H_2O in methanol + 0.05% TFA. Gradient 0→100%B over 60 mins. The fractions containing the peptide were evaporated under vacuum and then the peptide was freeze-dried from purified water. Purity was confirmed at 90% using analytical HPLC (ZORBAX Eclipse XBD-C18) (Mobile phase A: H_2O + 0.05% TFA. Mobile phase B: methanol + 0.05% TFA. Gradient 5→95%B over 20 mins) and the peptide mass was confirmed by MALDI mass spectrometry active W56 (M+Na, 1562) and (M+K, 1578), control F56 (M+Na, 1523) and (M+K, 1539).

2.3 Chemotaxis Assays

Cells were harvested and then re-suspended at a concentration of 25 x 10^4 cells mL^{-1} in serum-free RPMI 1640 containing 0.1% BSA. Cells were loaded in a total volume of 20 µL into the upper compartment of a microchemotaxis chamber (Receptor Technologies, Adderbury, UK) as described previously [5]). For inhibitor treatment, cells were incubated for 30 mins with the relevant inhibitors or vehicle control before loading onto the membrane. Chemoattractants at a concentration of 1 nM were loaded in a final volume of 31 µL at indicated concentrations in the lower compartment. The two compartments were separated by a polyvinylpyrollidone-free polycarbonate filter with 5 µm pores. The chemotaxis chamber was incubated at 37°C, 100% humidity, and 5% CO_2 for 4 hrs. The filter was then removed, and the number of cells migrating into each bottom compartment was counted using a haemocytometer. In all experiments, each data point was performed in duplicate.

2.4 Analysis of intracellular calcium ion concentration

MCF-7 cells were harvested and treated as described previously [29]. Cells were loaded with Fura-2 as described previously [30, 31]. Inhibitors were present during the 30 mins incubation period. Following incubation with inhibitors, cells were washed with calcium flux buffer and were re-suspended at 2×10^6 cells/mL in calcium flux buffer. Chemokine-induced intracellular calcium mobilisation was determined as described by Grynkiewicz [32] using a BMG Labtech Fluostar OPTIMA fluorometer. Chemokine was added after 15 secs of incubation in the fluorometer. Calcium mobilisation was monitored for a further 60 secs following chemokine challenge. Jurkat cells were harvested, then re-suspended in buffer as described [29]. Fluorescence was measured at 37°C every 3.5 secs. Stimulation with CXCL12 was after 30 secs. Calcium mobilisation and AUC was determined in a Flexstation III ROM V3.0.22 (Molecular Devices Ltd, Wokingham, UK) using SoftMax Pro and Excel, and displayed using GraphPad Prism.

2.5 Wound Healing Assays

MCF-7 cells were seeded onto 24 well plates overnight. After 24 hrs, the cells were washed once in DMEM without supplements and incubated in DMEM without supplements. A scratch was introduced to the monolayer with 200 µL pipette tips (time point 0). Inhibitors were added to the cells and incubated for 30 mins at 37°C, 100% humidity, and 5% CO_2. Chemokines or vehicle controls were added to the cells and pictures were taken at time point zero and after 24 hrs using an inverted Leica microscope. Images were analysed and the width of the wound was measured for control and with inhibitor treatment (with and without chemokine) at 0 hrs and 24 hrs. The ratio of the width of the wound after 24 hrs divided by the width of the

wound at 0 hrs was then used to compare the effectiveness of treatments in preventing migration, where a number of 1 denotes no migration and a number smaller than 1 denotes migration of cells.

2.6 Cell Viability Studies

MTS assays were performed using a CellTiter 96® AQueous Non-Radioactive Cell Proliferation Assay (Promega, Southampton, UK) and has been described previously [33] .

2.7 Internalisation assay and flow cytometry analysis

Jurkat T-cells were harvested, re-suspended at 5 x 10^5 cells/mL in 0.1% BSA/RPMI with inhibitors or control (H_2O) at either 37°C or 4°C for 30 mins, then treated with CXCL12 (15nM) at either 37°C or 4°C for 15 mins, washed with ice-cold 0.5% BSA/PBS, suspended in anti hCXCR4 clone 12G5 antibody from R&D Systems (1:2000) for 1 hr at 4°C, washed 3 times with ice-cold 0.5% BSA/PBS, then incubated for 1 hr at 4°C with fluorescein isothiocyanate (FITC)- conjugated anti-mouse IgG antibody (1:500). Stained cells were washed, gated to exclude dead cells using FSC versus SSC and quantified using a FACS Calibur, and data analysed using CellQuest software version 3.1 (Becton Dickinson, San Jose, CA).

2.8 cAMP Assay

cAMP assays were performed as recommended by manufacturers (Molecular Devices). Briefly, cells were harvested, re-suspended in 0.75 mM IBMX in Krebs-Ringer bicarbonate buffer (KRGB) pH7.4 at 2 x 10^6 cells/mL, treated with inhibitor or

control (H_2O) for 15 mins (37°C, 5%, CO_2), aliquots of 40 µL were treated with 20 µM forskolin for 15 mins (37°C, 5%, CO_2) before timed chemokine or H_2O control addition prior to lysis using CatchPoint buffers and protocols for cAMP analysis. Results were read at excitation 530 nm, emission 585 nm, cut off 570, using Flexstation III ROM v3.0.22.

2.9 Rac1 activation assays

Cells were serum starved for 24 hrs, treated at 37°C with inhibitors for 30 mins then 10 nM CXCL12 for 15 mins, lysed (50 mM Tris pH 7.5, 10 mM $MgCl_2$, 0.5 M NaCl, 2% Igepal) and 800 µg protein/sample used in Rac1 Activation Assay, with 10 µg protein/sample for total rac, following Rac1 Activation Assay Biochem Kit protocol (Cytoskeleton Inc). The samples were separated on a 10% SDS-PAGE and electrophoretically transferred to a nitro-cellulose membrane. The membranes were blocked with 5% non-fat powdered milk in PBS (30 mins, RT). For Western blotting, these membranes were incubated at 4°C overnight with 1:500 anti-Rac1 antibody, ARC03, in TBST, no blocker, then rinsed 50 mL TBST (1 min) and then incubated with 1:10,000 goat anti-mouse HRP conjugate in TBST (1 hr, RT) membrane washed with TBST (5x10 mins). The blots were developed using PierceTM ECL western blotting substrate (ThermoFisher Scientific)

2.10 Analysis of data

Data were analysed using GraphPad Prism V6 (GraphPad Software). Statistical analyses were performed using a One-way ANOVA with post-hoc Bonferroni or Tukey's multiple comparisons tests. Data represent the mean ± SEM of at least three independent experiments.

3. Results

3.1 CXCL12-induced chemotaxis in Jurkat and THP-1 cells is blocked by Rac1 GEF inhibitor NSC23766

We set out to examine the role of Rac1 in chemokine-induced cell chemotaxis for different receptors and cell types. Whereas there was no inhibitory effect on CCL3-induced chemotaxis after pre-treatment of THP-1 cells with NSC23766, a specific Rac1-GEF interaction inhibitor [34] (Figure 1a), there was, however, a significant reduction of chemotaxis towards CXCL12 (Figure 1b). We confirmed the inhibitory effect of NSC23766 on CXCL12 chemotaxis in Jurkat cells (Figure 1c), where virtually no cells migrated after NSC23766 treatment, whereas in THP-1 cells about 40% of migration was observed. Cell viability assays (MTS assays) showed that over the timeframe and concentrations used, NSC23766 exhibits only a minor toxic effect on cell growth (data not shown). The Rac1 inhibitor EHT1864 gave similar results, blocking significantly CXCL12 induced chemotaxis (Figure 1 d), but not CCL3 induced chemotaxis. (Figure 1e). We also used the CXCR4 specific orthosteric antagonist AMD3100, to block chemotaxis in our assay (Figure 1f). AMD3100 is a bicyclam antagonist of CXCR4 thought to bind three acidic residues Asp^{171}, Asp^{262} and Glu^{288} in the main binding pocket of CXCR4 [35]. In contrast ATI2341 is an allosteric agonist derived from a CXCR4 intracellular loop 1 protein sixteen residue sequence. ATI2341 has many rotatable bonds facilitating flexible docking and a long palmitate tail facilitating cell penetration. ATI2341 had a small non-significant

negative effect on CXCL12 induced chemotaxis in Jurkat cells (Figure 1g). When used on their own, neither NSC23766, nor AMD3100 or ATI2341 induced any chemotactic responses in Jurkat cells (Figure 1h).

3.2 A Rac1 inhibitory peptide also blocks CXCL12 induced chemotaxis, but not CCL3 in THP-1 and Jurkat cells

Small molecule inhibitors can have off-target effects and indeed it has been described that NSC23766 has additional effects on muscarinic acetylcholine receptors, where it acts a competitive antagonist [36]. We therefore synthesized a previously described peptide (W56) [37] which targets a sequence in the β3 region of switch 2 in Rac1 and blocks its functionality (Figure 2a). As an internal control we used an inactive control peptide (F56), which has a key amino acid, tryptophan, substituted by phenylalanine to inactivate the peptide. Even at very high concentrations, this W56 peptide did not show any toxicity in THP-1 cells (Figure 2b). We repeated the chemotaxis assays in THP-1 and Jurkat cells in the presence or absence of the Rac1-binding peptide (W56) and we confirmed the peptide's inhibitory effect on CXCL12-induced chemotaxis, whereas there was no effect on CCL3-induced chemotaxis (Figure 2c,d). Similarly in Jurkat cells, the Rac1-binding peptide (W56) blocked CXCL12-induced chemotaxis in THP-1 cells (Figure 2e). The inactive F56 peptide did not block CXCL12 or CCL3 chemotaxis (Figure 2). Increasing the concentration of W56 to 560 µM does not change the differences observed between the two chemokines tested (data not shown).

3.3 Rac1 inhibition blocks CXCL12-induced migration of adherent MCF-7 cells

We previously observed differences in the signalling machinery utilised during cell migration with regards to adherent cells compared to suspension cells [5]. To analyse whether the use of Rac1 differs in suspension versus adherent cells, we used a cellular model of wound healing assays in the adherent breast cancer line MCF-7. Since wound healing assays expose the cells towards the drugs for a longer timeframe than a chemotaxis assay does, we repeated the MTS cell viability assay for NSC23766 on MCF-7 cells (Figure 3a), selecting the 25 µM dosage to treat the cells, and we used the peptide concentration of 280 µM for W56 and F56. Rac1 activation assays showed that CXCL12 leads to activation of Rac1 in MCF-7 cells, which can be blocked by the Rac1 GEF inhibitor NSC23766 as well as by the CXCR4 antagonist AMD3100 and the allosteric agonist ATI2341 (Figure 3b). The results of the wound healing assays mirror the results in suspension cells. Neither the active W56 peptide nor NSC23766 blocked CCL3-induced migration (Figure 3c), whereas the active W56 peptide as well as NSC23766 blocked migration in response to CXCL12 (Figure 3d). These results clearly show that in CCL3-induced migration compared with CXCL12-induced migration Rac1 activation is not necessary.

3.4 NSC23766 acts as a competitive antagonist in CXCL12-induced chemotaxis in Jurkat cells

To understand the action of NSC23766 in more detail, we performed a concentration response curve for CXCL12-induced chemotaxis in Jurkat cells in the presence or absence of 50 µM NSC23766. We used a slightly lower concentration of NSC23766 as compared to our initial experiments, in order not to prevent migration completely (Figure 4a left). The sigmoidal dose response curves clearly show a

reduction in potency in the presence of NSC23766 (EC_{50} of CXCL12 in the absence of NSC23766: 0.19 nM, in the presence of NSC23766 the EC_{50} for CXCL12 is 2 nM), but there is no effect on the efficacy of CXCL12. De facto NSC23766 behaves like a competitive antagonist for CXCR4 in this assay and the inhibitory response is surmountable. We did further experiments in the presence of different concentrations of NSC23766 and plotted the data as Schild plot which allowed the calculation of the pA2 for NSC23766, which is 5.2 (Figure 4a, right)and used a Gaddum/Schild EC_{50} shift to calculate the affinity as well, which is determined at 4 µM. The CXCR4-specific antibody 12G5 is capable of blocking chemotaxis [38]. At 50 and 25 µM concentration of NSC23766 there is an additive effect of NSC23766 treatment on inhibition of CXCL12-induced chemotaxis in the presence of the 12G5 antibody, whereas at the lower concentration of NSC23766, no significant additive effect on 12G5 occurs (Figure 4b). At 100 µM concentration of NSC23766 the addition of 12G5 has no effect on further reducing chemotaxis. A similar effect can be seen with the allosteric agonist ATI2341, but not with AMD3100 (Figure 4c). This data leads us to speculate that the action of NSC23766 in this system is not solely blocking the Rac1-GEF interaction, but is also acting on the CXCR4 receptor directly.

3.5 NSC23766 blocks CXCL12-induced calcium release in THP-1 and Jurkat cells

NSC23766 does not block CCL3-induced release of calcium in THP-1 (Figure 5a), and has therefore no general effect on cell signalling. In contrast, we observed a significant reduction in calcium release after CXCL12 activation in THP-1 cells which have been pre-treated with NSC23766. Again, these results point to NSC23766 having additional effects on CXCR4 rather than solely blocking Rac1-GEF (Figure

5b). The Rac1 inhibitor EHT 1864 does not inhibit the release of calcium in these cells for both CXCL12 as well as CCL3. Intracellular calcium responses to CXCL12 in Jurkat cells pre-treated with AMD3100, NSC23766 or ATI2341 illustrate that ATI2341 clearly increases total calcium release, whereas AMD3100 and NSC23766 dramatically reduce calcium release in this cell line (Figure 5c). This alludes to the fact that ATI2341 acts as a CXCR4 agonist with respect to calcium release, whereas both AMD3100 and NSC23766 dramatically reduced the AUC compared to control and act as antagonists (see Figure 5c).

The addition of CXCL12 for 15 mins before staining with the CXCR4 specific antibody leads to rapid internalisation of the receptor from the surface of Jurkat cells, which is measurable by a loss of fluorescence (Figure 6a, b). Cells that were pre-incubated with NSC23766 exhibited a similar profile after 12G5 staining as cells where the receptor has been internalised (Figure 6b), whether they have been subjected to CXCL12 treatment or not. This apparent loss of receptors could occur if Rac1 inhibition triggers receptor internalisation even if the receptor is inactive, or it could occur due to the NSC23766 competitively binding to the monoclonal antibody binding sites. It could also be due to a conformational change in the receptor which leads to a loss on antibody binding, as has been proposed by Zoughlami et al. [26]. We therefore repeated the CXCR4 internalisation experiments with the active (W56) and inactive control (F56) peptides. We did not observe any significant effects on receptor expression or internalisation (Figure 6b). This makes it highly unlikely that general Rac1 inhibition triggers internalisation or leads to a conformational change which leads to a loss of antibody binding. We hypothesized that if NSC23766 was competing with the 12G5 antibody to bind to the receptor, then the same experiment performed at 4°C to prevent active internalisation of CXCR4, would show the same

results as experiments performed at 37°C, where the receptor can undergo internalisation (modelling of NSC interaction with CXCR4 is supplied in the Supporting information section). This is in fact what our data shows (Figure 6c), suggesting that NSC23766 is not acting via receptor internalisation. Furthermore, treatment with NSC23766 following primary and secondary antibody treatment produced a greater loss of receptor 12G5 staining than pre-treatment with NSC23766 before receptor staining (Figure 6c). This suggests that although NSC23766 rapidly binds CXCR4, its affinity weakens over the timescale of the receptor staining (about 2 hrs) (Figure 6c).

To verify these results we also treated Jurkat cells with AMD3100 and ATI2341 (Figure 7a). The results show that ATI2341 (5μM) does not induce internalisation on its own, and it does not block CXCL12-induced internalisation. AMD3100 binds to the same site on CXCR4 as the 12G5 antibody and is known to prevent antibody binding, and therefore exhibited a similar result as NSC23766 at 37°C (Figure 6b and 7a). However we found that the effects of 100 μM NSC23766 are considerably more pronounced than those of 5 μM AMD3100 at 4°C (Figure 6c).

CXCR4 receptors couple to Gαi/o heterotrimeric G proteins, so therefore we treated Jurkat cells with forskolin to induce cAMP production after pre-treating the cells with either NSC23766, AMD3100, ATI2341 or H89 (a potent, cell-permeable protein kinase A (PKA) inhibitor). 10 mins activation of CXCR4 receptors with CXCL12 leads to a loss of quantifiable cAMP in the cells, which is not blocked by AMD3100, ATI2341 or H89. NSC23766 induces a reduction in cAMP levels in the absence of CXCR4 receptor activation, which is then increased by the addition of CXCL12 (Figure 7b), suggesting that NSC23766 may also act as a CXCR4 agonist, which can induce reduction in cAMP production, but is not capable of inducing cell

chemotaxis. Alternatively, NSC23766 acts an agonist at a receptor distinct from CXCR4 and their effects are cumulative.

4. Discussion

Chemokine receptor-induced cell chemotaxis is a crucial step in metastasis of cancer as well as the inflammatory response [12]. The chemokine receptor CXCR4 has been of interest for a number of years, as it has been shown to be up-regulated in several cancers and its activation can lead to cancer cell metastasis [7-9, 25, 39-41]. Although different studies investigated how CXCL12-induced activation of CXCR4 leads to chemotaxis of cells, there are still many unanswered questions. We have shown recently that the type of cells where the receptor is expressed has an effect on which downstream signalling partners will be utilised to transduce the signal from receptor towards cell migration [5]. Also there are distinct differences in which pathways are used, depending on which receptor becomes activated [5, 29]. We therefore set out to investigate how Rac1 signalling is involved with chemotaxis towards CXCL12 or CCL3 in different cell types. One of the findings in our study is that there are indeed differences in whether Rac1 activation is essential for cell chemotaxis or not. CCL3-induced chemotaxis occurs in the absence of Rac1 activation, in both suspension and adherent cell types, whereas CXCL12 chemotaxis is completely prevented when Rac1 is blocked by a specific Rac1 binding peptide or by the Rac1 inhibitor EHT 1864. This in contrast to previous studies in chronic lymphocytic leukaemia (CLL) cells, where chemotaxis towards CXCL12 relied on RhoA activation and not Rac1, which again highlights the important impact different cell types have on receptor-induced signalling [23].

Our results with the Rac1-GEF inhibitor NSC23766 are more complicated. Using NSC23766 we confirmed that CCL3-induced chemotaxis in THP-1 cells as well as MCF-7 cells occurs independently of Rac1 activation. On first sight, the data also confirms that CXCL12-induced chemotaxis is completely reliant on Rac1 activation, however, there are more dimensions to these results. Recently it has been shown that NSC23766 indeed acts as antagonist on various receptors [36, 42]. NSC23766 can directly regulate NMDA receptors as indicated by their strong effects on both exogenous and synaptically evoked NMDA, indicating that NSC23766 could be a novel NMDA receptor antagonist [42]. Similarly, NSC27366 inhibits the M2 muscarinic acetylcholine receptor (M2 mAChR) and induces a concentration-dependent rightward shift of the carbachol concentration response curves at all mAChRs [36]. There have also been studies showing that Rac1 can lead to a direct conformational change in CXCR4 and that Rac1 inhibition affects this as well [26]. With this in mind, we investigated the role of NSC27366 in CXCL12-induced chemotaxis further. Concentration response curves in the presence or absence of NSC23766 clearly showed a shift in potency for CXCL12 in the presence of NSC23766, with no effect on the overall efficacy of the chemokine, which points to NSC23766 being a competitive antagonist on CXCR4 and not to NSC23766 solely blocking Rac1 activation, which was also confirmed with a Gaddum/Schild EC_{50} shift analysis. 12G5, a CXCR4 antibody which has been shown to be dependent on receptor conformation for binding [43], can block chemotaxis of cells. In our hands there is a clear additive effect of NSC23766 and 12G5; together they block chemotaxis to greater extent than either on their own. The allosteric agonist ATI2341, which has been shown to induce chemotaxis via CXCR4 in polymorphonuclear neutrophils (PMNs) but not in lymphocytes [44], does not induce

chemotaxis in Jurkat cells, but has a slight inhibitory effect on CXCL12-induced chemotaxis, acting like a weak partial agonist. This effect is synergistic with the effects seen with NSC23766, whereas AMD3100 and NSC23766 do not exhibit any synergistic effect. ATI2341 has been shown to have a very weak effect on CXCR4 internalisation [45], which we can confirm. It does not affect CXCL12-induced internalisation, nor is there any effect visible in cAMP assays, even though ATI2341 has been shown to engage Gαi heterotrimeric G proteins [45]; however we recognise an increase in overall calcium release in the cells in the presence of ATI2341, even if the peak release is not higher.

Unlike previous publications who linked expression levels of CXCR4 directly to the functionality of Rac1 [26], we observed further effects of NSC27366 in these experiments. Our data points to NSC27366 directly binding to CXCR4, as has been shown for other receptors [36, 42] and inducing diverse signalling (see supporting information). We have previously shown that the chemokine receptor signalling can differ depending on cell types used [5], and therefore it is not too surprising that data recorded in transfected HEK293 [26] cells do not match with cAMP assays in Jurkat cells, where a reduction in cAMP levels after NSC23766 treatment can be observed, which is further decreased by the addition of CXCL12 (Figure 7 b). These results do not necessarily disagree with the hypothesis that Rac1 blockade leads to a conformational change in CXCR4, however it would be an active conformation of the receptor and not an inactive conformation. NSC23766 can lead to the downregulation of receptors from the cell surface as has been shown for glycoprotein on platelets [46]. Our data with the W56 peptide in Jurkat cells show internalisation of CXCR4, and not a conformational change, since only in the presence of CXCL12 is there a loss of receptor expression, whereas a

conformational change would show this loss in the absence of agonist as well. We also cannot confirm the Rac1 inhibition is essential for CXCR4-induced internalisation, since even in the presence of W56, the receptor internalises after activation with CXCL12.

The concept of biased agonism has become more popular within the chemokine field, since increasingly numerous examples from the field of GPCRs point to the fact that structurally different ligands acting on the same receptor can activate different signalling pathways within the cell [47-49]. An agonist may preferentially stabilize a receptor conformation over another, leading to the recruitment of a particular group of intracellular signalling molecules to the receptor and the preferential activation of one downstream signalling pathway over another [50]. Overall our data points to NSC23766 directly binding to CXCR4 and inducing specific signalling events which differ from CXCL12, and therefore confirms the concept of ligand biased signalling on the CXCR4 receptor.

Acknowledgments

We acknowledge the support for SCM from the Novartis studentship fund.

Authorship Contribution

Contribution: S.C.M designed and performed the experiments, analysed, and interpreted the data, and wrote the manuscript; L.H. and L.S. performed some experiments; A.B. did the molecular modelling; A.M. supervised the study, designed the experiments, analysed and interpreted the data, and wrote the manuscript.

Conflict-of-interest disclosure: The authors declare no competing financial interests.

5. References

[1] Thelen M, Nat Immunol. 2001;2:129-134.
[2] Homey B, Muller A, Zlotnik A, Nat Rev Immunol. 2002;2:175-184.
[3] Zlotnik A, Ernst Schering Res Found Workshop. 2004:53-58.
[4] Dillenburg-Pilla P, Patel V, Mikelis CM, Zarate-Blades CR, Doci CL, Amornphimoltham P, Wang Z, Martin D, Leelahavanichkul K, Dorsam RT, Masedunskas A, Weigert R, Molinolo AA, Gutkind JS, FASEB J. 2015;29:1056-1068.
[5] Mills SC, Goh PH, Kudatsih J, Ncube S, Gurung R, Maxwell W, Mueller A, Cell Signal. 2016;28:316-324.
[6] Vaday GG, Peehl DM, Kadam PA, Lawrence DM, Prostate. 2006;66:124-134.
[7] Zlotnik A, Int J Cancer. 2006;119:2026-2029.
[8] Zlotnik A, Semin Cancer Biol. 2004;14:181-185.
[9] Balkwill F, Semin Cancer Biol. 2004;14:171-179.
[10] Li Y, Wu J, Zhang P, Tumour biology : the journal of the International Society for Oncodevelopmental Biology and Medicine. 2016;37:4501-4507.
[11] Delgado-Martin C, Escribano C, Pablos JL, Riol-Blanco L, Rodriguez-Fernandez JL, J Biol Chem. 2011;286:37222-37236.
[12] Bachelerie F, Ben-Baruch A, Burkhardt AM, Combadiere C, Farber JM, Graham GJ, Horuk R, Sparre-Ulrich AH, Locati M, Luster AD, Mantovani A, Matsushima K, Murphy PM, Nibbs R, Nomiyama H, Power CA, Proudfoot AE, Rosenkilde MM, Rot A, Sozzani S, Thelen M, Yoshie O, Zlotnik A, Pharmacological reviews. 2014;66:1-79.
[13] Blanpain C, Migeotte I, Lee B, Vakili J, Doranz BJ, Govaerts C, Vassart G, Doms RW, Parmentier M, Blood. 1999;94:1899-1905.
[14] Mueller A, Kelly E, Strange PG, Blood. 2002;99:785-791.
[15] Germena G, Hirsch E, Mol Immunol. 2013;55:83-86.
[16] Kerr JS, Jacques RO, Moyano Cardaba C, Tse T, Sexton D, Mueller A, Cell Signal. 2013;25:729-735.
[17] Ridley AJ, Curr Opin Cell Biol. 2015;36:103-112.
[18] Pollard TD, Borisy GG, Cell. 2003;112:453-465.
[19] Ridley AJ, Methods Mol Biol. 2012;827:3-12.
[20] Mueller A, Strange PG, Eur J Biochem. 2004;271:243-252.
[21] Ryan CM, Brown JA, Bourke E, Prendergast AM, Kavanagh C, Liu Z, Owens P, Shaw G, Kolch W, O'Brien T, Barry FP, Stem Cell Res Ther. 2015;6:136.
[22] Cross AK, Richardson V, Ali SA, Palmer I, Taub DD, Rees RC, Cytokine. 1997;9:521-528.
[23] Hofbauer SW, Krenn PW, Ganghammer S, Asslaber D, Pichler U, Oberascher K, Henschler R, Wallner M, Kerschbaum H, Greil R, Hartmann TN, Blood. 2014;123:2181-2188.
[24] Li H, Yang L, Fu H, Yan J, Wang Y, Guo H, Hao X, Xu X, Jin T, Zhang N, Nat Commun. 2013;4:1706.
[25] Guo J, Yu X, Gu J, Lin Z, Zhao G, Xu F, Lu C, Ge D, Tumour biology : the journal of the International Society for Oncodevelopmental Biology and Medicine. 2016;37:6371-6378.
[26] Zoughlami Y, Voermans C, Brussen K, van Dort KA, Kootstra NA, Maussang D, Smit MJ, Hordijk PL, van Hennik PB, Blood. 2012;119:2024-2032.
[27] Moyano Cardaba C, Jacques RO, Barrett JE, Hassell KM, Kavanagh A, Remington FC, Tse T, Mueller A, Biochem Biophys Res Commun. 2012;418:17-21.
[28] Malkinson JP, Zloh M, Kadom M, Errington R, Smith PJ, Searcey M, Org Lett. 2003;5:5051-5054.

[29] Jacques RO, Mills SC, Cazzonatto Zerwes P, Fagade FO, Green JE, Downham S, Sexton DW, Mueller A, Cell Biochem Funct. 2015;33:407-414.
[30] Cardaba CM, Mueller A, Biochem Pharmacol. 2009;78:974-982.
[31] Cardaba CM, Kerr JS, Mueller A, Cell Signal. 2008;20:1687-1694.
[32] Grynkiewicz G, Poenie M, Tsien RY, J Biol Chem. 1985;260:3440-3450.
[33] Khabbazi S, Jacques RO, Moyano Cardaba C, Mueller A, Cell Biochem Funct. 2013;31:312-318.
[34] Gao Y, Dickerson JB, Guo F, Zheng J, Zheng Y, Proc Natl Acad Sci U S A. 2004;101:7618-7623.
[35] Rosenkilde MM, Gerlach LO, Jakobsen JS, Skerlj RT, Bridger GJ, Schwartz TW, J Biol Chem. 2004;279:3033-3041.
[36] Levay M, Krobert KA, Wittig K, Voigt N, Bermudez M, Wolber G, Dobrev D, Levy FO, Wieland T, J Pharmacol Exp Ther. 2013;347:69-79.
[37] Gao Y, Xing J, Streuli M, Leto TL, Zheng Y, J Biol Chem. 2001;276:47530-47541.
[38] Yang H, Lan C, Xiao Y, Chen YH, Immunol Lett. 2003;88:27-30.
[39] Teicher BA, Fricker SP, Clinical cancer research : an official journal of the American Association for Cancer Research. 2010;16:2927-2931.
[40] Liekens S, Schols D, Hatse S, Current pharmaceutical design. 2010;16:3903-3920.
[41] Sun Y, Mao X, Fan C, Liu C, Guo A, Guan S, Jin Q, Li B, Yao F, Jin F, Tumour biology : the journal of the International Society for Oncodevelopmental Biology and Medicine. 2014;35:7765-7773.
[42] Hou H, Chavez AE, Wang CC, Yang H, Gu H, Siddoway BA, Hall BJ, Castillo PE, Xia H, J Neurosci. 2014;34:14006-14012.
[43] Baribaud F, Edwards TG, Sharron M, Brelot A, Heveker N, Price K, Mortari F, Alizon M, Tsang M, Doms RW, J Virol. 2001;75:8957-8967.
[44] Tchernychev B, Ren Y, Sachdev P, Janz JM, Haggis L, O'Shea A, McBride E, Looby R, Deng Q, McMurry T, Kazmi MA, Sakmar TP, Hunt S, 3rd, Carlson KE, Proc Natl Acad Sci U S A. 2010;107:22255-22259.
[45] Quoyer J, Janz JM, Luo J, Ren Y, Armando S, Lukashova V, Benovic JL, Carlson KE, Hunt SW, 3rd, Bouvier M, Proc Natl Acad Sci U S A. 2013;110:E5088-5097.
[46] Dutting S, Heidenreich J, Cherpokova D, Amin E, Zhang SC, Ahmadian MR, Brakebusch C, Nieswandt B, J Thromb Haemost. 2015;13:827-838.
[47] Steen A, Larsen O, Thiele S, Rosenkilde MM, Front Immunol. 2014;5:277.
[48] Zweemer AJ, Toraskar J, Heitman LH, AP IJ, Trends Immunol. 2014;35:243-252.
[49] Anderson CA, Solari R, Pease JE, J Leukoc Biol. 2016;99:901-909.
[50] Kenakin T, Br J Pharmacol. 2015;172:4238-4253.

6. Figures legends

Figure 1: **NSC23766 blocks CXCL12-induced chemotaxis but not CCL3**. A) Shows migratory response of THP-1 cells towards 1 nM CCL3 in untreated control cells or 100 µM NSC23766 pre-treated cells. B) Cell chemotaxis towards 1 nM

CXCL12 in untreated control cells or 100 µM NSC23766 pre-treated THP-1 cells. C) Cell chemotaxis towards 1 nM CXCL12 in untreated control cells or 100 µM NSC23766 pre-treated Jurkat cells. D) Cell chemotaxis towards 1 nM CXCL12 in untreated control cells or 100 nM EHT1864 pre-treated Jurkat cells. E) Cell chemotaxis towards 1 nM CCL3 in untreated control cells or 100 nM EHT1864 pre-treated THP-1 cells. F) Cell chemotaxis towards 1 nM CXCL12 in untreated control cells or 1 µM AMD3100 pre-treated Jurkat cells, G) Cell chemotaxis towards 1 nM CXCL12 in untreated control cells or 5 µM ATI23415 pre-treated Jurkat cells. H) Cell chemotaxis towards 1 nM CXCL12 or towards NSC23766, AMD3100 or ATI23415 as chemoattractants. Data shown are the mean ± SEM of at least 3 independent experiments. (* = p≤0.05, *** = p≤0.001, One-way ANOVA with a Tukey's multiple comparisons test as post-test).

Figure 2: **Rac1 activation is essential for CXCL12-**induced chemotaxis **but not for CCL3**.

A) Shows amino-acid sequence of active W56 peptide and inactive control F56 peptide, * denotes C-terminal amide, B) MTS assays in THP-1 cells showing no toxicity against different peptide concentrations. C) Shows migratory response of THP-1 cells towards 1 nM CXCL12 in untreated control cells, inactive F56 or active W56 pre-treated cells. D) Cell chemotaxis towards 1 nM CCL3 in untreated control cells, inactive F56 or active W56 pre-treated THP-1 cells. E) Shows migratory response of Jurkat cells towards 1 nM CXCL12 in untreated control cells, inactive F56 or active W56 pre-treated cells. Data shown are the mean ± SEM of at least 3 independent experiments. (** = p≤0.01, *** = p≤0.001, One-way ANOVA with a Tukey's multiple comparisons test as post-test).

Figure 3: **Rac1 activation is essential for CXCL12-induced migration of MCF-7 cells.** A) Shows MTS assay with 25 µM NCS27366 and 280 µM W56 or F56 over 48 hrs, B) Rac1 activation assay in the presence/absence of CXCL12 and AMD3100, ATI2341, NSC23766, upper panel shows active Rac1, lower panel shows total Rac1 in lysate. C) Wound healing assay on MCF-7 cells after treatment with NSC23766, inactive F56 or active W56. Cell migration was induced with 10 nM CCL3 and measured after 24 hrs. Left side shows quantified migration, right shows representative pictures from scratch D) Wound healing assay on MCF-7 cells after treatment with NSC23766, inactive F56 or active W56. Cell migration was induced with 10 nM CXCL12 and measured after 24 hrs. Left side shows quantified migration, right shows representative pictures from scratch. Quantification of migration of cells into the wound: A number of 1 denotes no migration occurred whereas a number < 1 denotes cell migration. ** denotes a significant difference towards the corresponding control (***=p≤0.001, One-way ANOVA with a Tukey's multiple comparisons test as post-test). Data shown are the mean ± SEM of 3 independent experiments, western blot analysis shows initial data from experiments.

Figure 4: **NSC23766 changes potency of CXCL12 in chemotaxis assays and has an additive effect on the neutralising 12G5 antibody and ATI2341, but not on AMD3100**. A) Figure on left shows a concentration response curve towards CXCL12 in untreated control cells or 50 µM NSC23766 pre-treated Jurkat cells, right shows a Schild plot analysis in the presence of different concentrations of NSC23766. B) Shows chemotaxis towards 1 nM CXCL12 in Jurkat cells where cells have been either left untreated, pre-treated with 12G5 (1:2000) or different

concentration of NSC23766 or both of them. C) Shows chemotaxis towards 1 nM CXCL12 in Jurkat cells were cells have either been treated with 50 µM NSC23766, 5 µM ATI2341, 0.5 µM AMD3100 or a combination of NSC23766/ATI2341 or NSC23766/AMD3100. Data shown are the mean ± SEM of 3 independent experiments. (*** = p≤0.001, One-way ANOVA with a Tukey's multiple comparisons test as post-test).

Figure 5: NSC23766 does not affect the release of intracellular calcium in response to CCL3 activation in THP-1 cells. A) Figure on left, stimulation of untreated, NSC23766 or EHT 1864 treated THP-1 cells with CCL3 100 nM leads to release of intracellular calcium, on the right representative trace showing stimulation of untreated or NSC23766 treated cells with CCL3 100 nM. B) Left figure, stimulation of untreated, NSC23766 or EHT1 1864 treated THP-1 cells with CXCL12 10nM leads to release of intracellular calcium, on the right representative trace showing stimulation of untreated or NSC23766 treated cells with CXCL12 10 nM. C) Left figure, stimulation of untreated or NSC23766, AMD3100 and ATI2341 treated Jurkat cells with CXCL12 10nM leads to release of intracellular calcium, on the right representative trace showing stimulation of untreated or inhibitor treated cells. A, B: Data in single traces were normalised to stimulation over basal. (** = p≤0.01, paired Student’s t-test, n=3), C: Area under the curve was calculated using SoftMax Pro and Excel (*** = p≤0.001, * = p≤0.05, One-way ANOVA with a Tukey's multiple comparisons test as post-test, n=6).

Figure 6: NSC23766 acts an agonist and leads to internalisation of CXCR4. A) Flow cytometry analysis of CXCR4 expression on Jurkat cells in either control cells

or pre-treated cells: solid black is the negative control, black line is the positive 12G5 control, green line are control cells treated with CXCL12, blue line are cells treated with NSC23766 100μM, red line are cells treated with NSC23766 and CXCL12, B) cells were pre-incubated with inhibitors for 30 mins at 37°C and internalisation of CXCR4 was induced with CXCL12 15 nM. Cells were then stained for CXCR4 expression and analysed using flow cytometry. Data is presented as mean plus S.E.M. of the mean fluorescence measured of 4 independent experiments C) Cells were kept at 4°C for all incubation steps. Cells were either pre-incubated with inhibitors before induction of internalisation and the antibody stain or the cells were stained with 12G5 first and then incubated with inhibitors (post NSC23766, post AMD3100, post ATI2341 4°C, 30 mins). Data is presented as mean plus S.E.M. of the mean fluorescence measured of at least 6 independent experiments

Figure 7: ATI2341 does not induce internalisation of CXCR4, NSC23766 acts as an agonist on CXCR4 in cAMP assays. A) Data shows levels of CXCR4 expression in Jurkat cells in control, AMD3100 or ATI2341 pre-treated cells in response to CXCL12 activation. Data shown are the mean ± SEM of 3 independent experiments. (*** = p≤0.001, One-way ANOVA with a Tukey's multiple comparisons test as post-test). B) Data show levels of cAMP in Jurkat cells after treatment with 100 nM CXCL12 for 10 mins. Cells were pre-treated with 20 mM forskolin to induce cAMP production and either NSC23766, AMD3100, ATI2341, H89 or left untreated for 30 mins before they were incubated with 100 nM CXCL12 for 10 mins and the amount of cAMP present was measured using a CatchPoint cAMP Fluorescent Assay Kit. Data shown are the mean ± SEM of 4 independent experiments. (*** = p≤0.001, One-way ANOVA with a Tukey's multiple comparison tests as post-test)

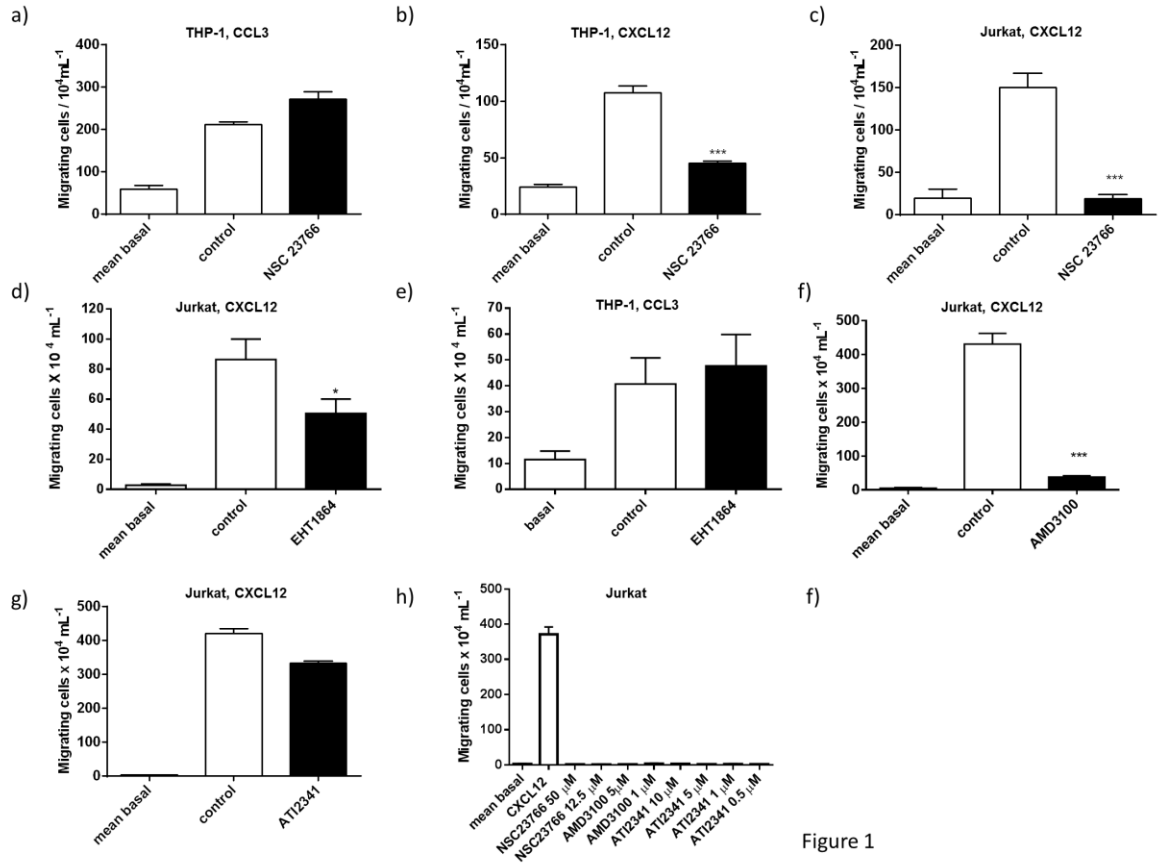

Figure 1

a)

W56: Val-Asp-Gly-Lys-Pro-Val-Asn-Leu-Gly-Leu-Trp-Asp-Thr-Ala-Gly*

F56: Val-Asp-Gly-Lys-Pro-Val-Asn-Leu-Gly-Leu-Phe-Asp-Thr-Ala-Gly*

b)

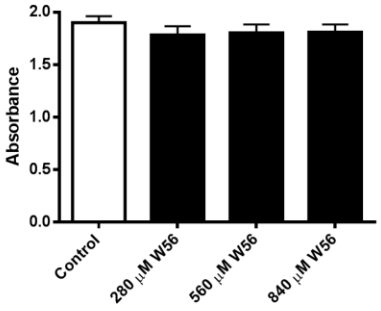

c)

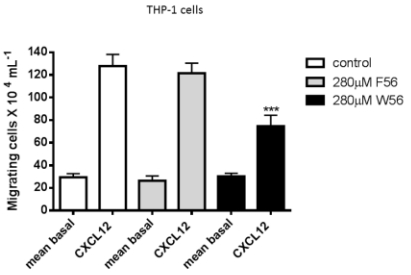

d)

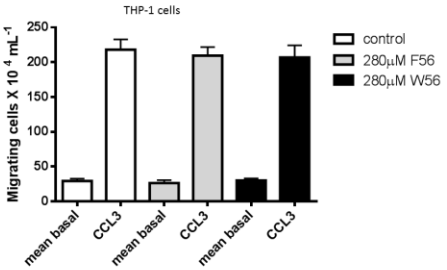

e)

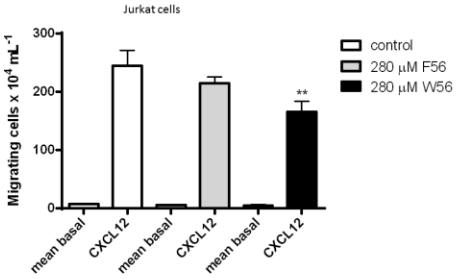

Figure 2

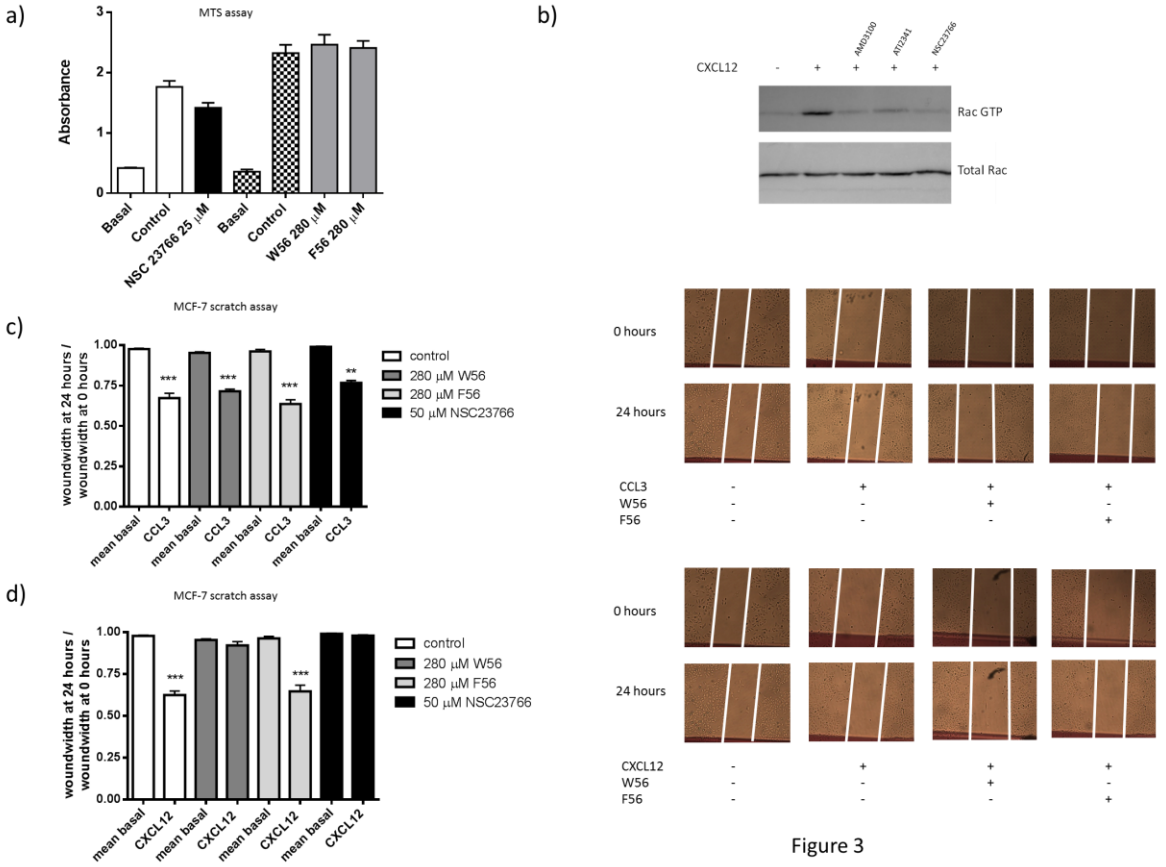

Figure 3

Figure 4

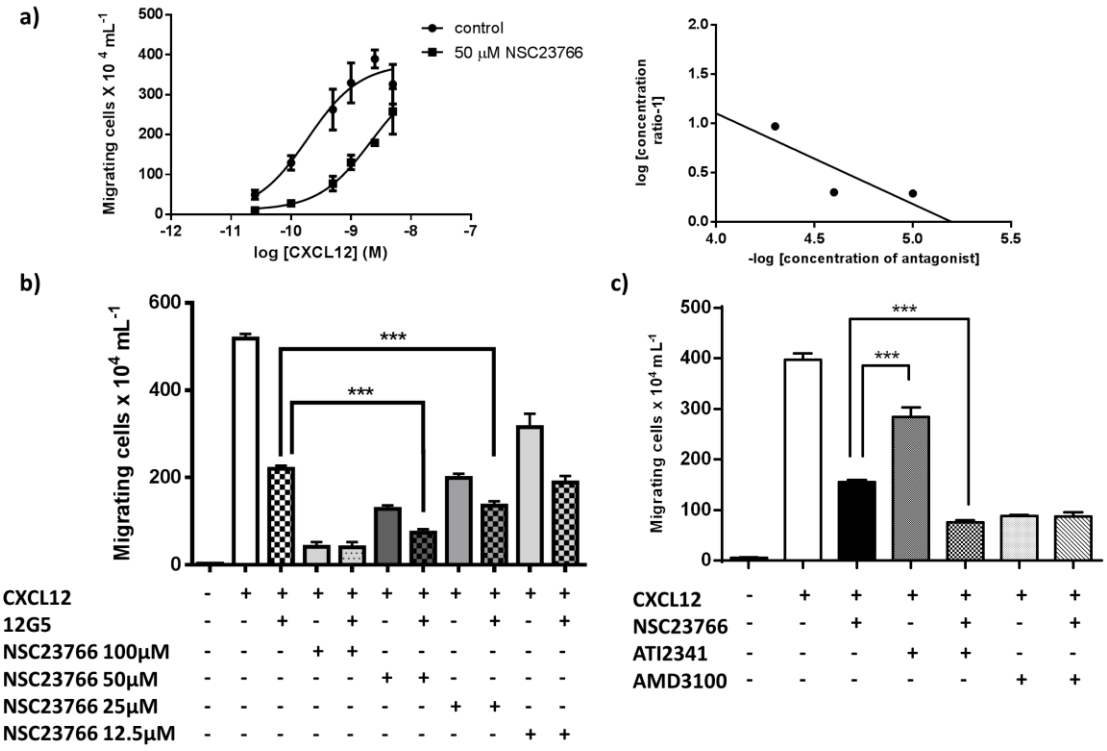

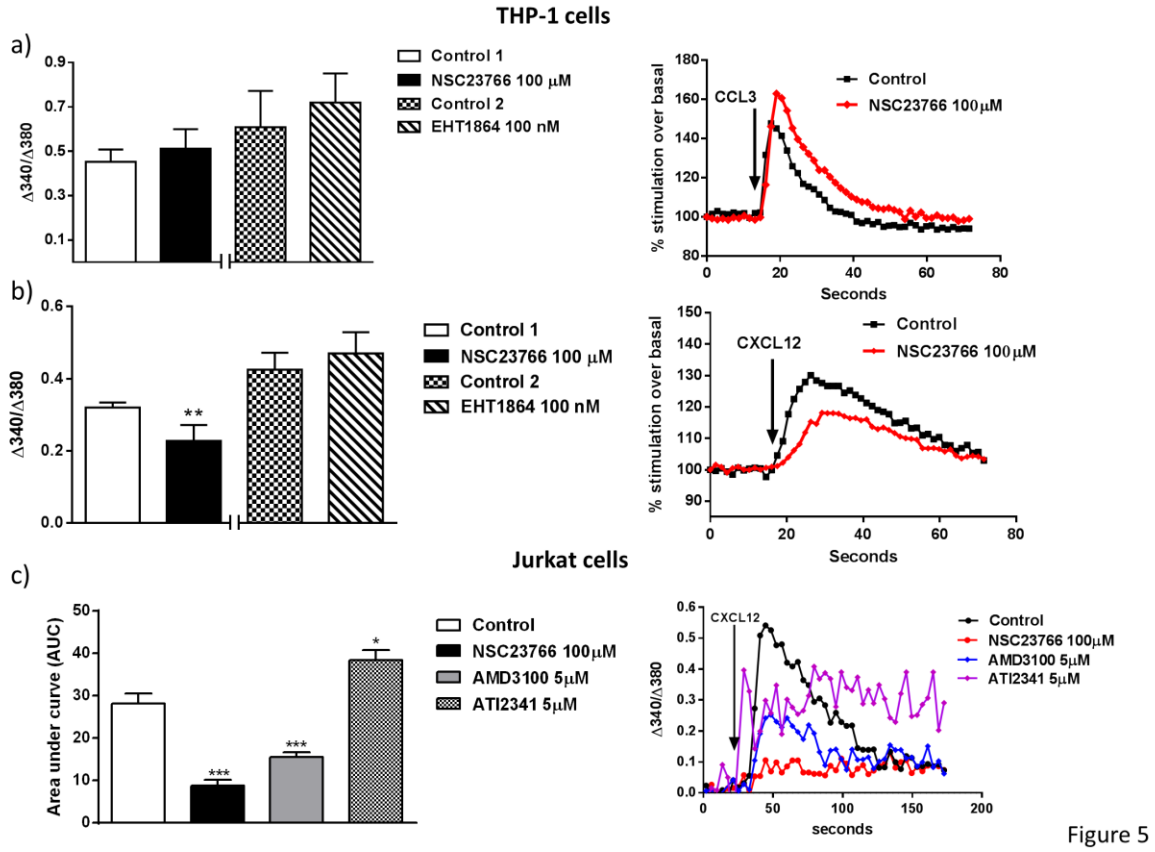

Figure 5

a)

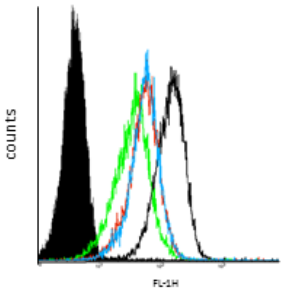

Solid black: negative control
Black: positive control
Green: CXCL12
Blue: NSC23766
Red:NSC23766 + CXCL12

b)

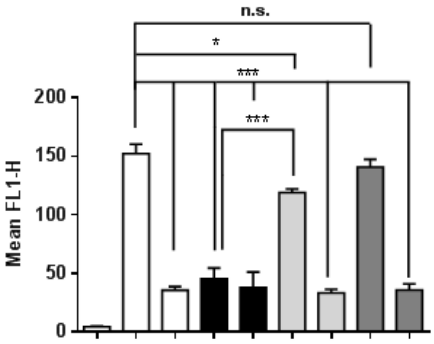

12G5	-	+	+	+	+	+	+	+	+
CXCL12	-	-	+	-	+	-	+	-	+
NSC23766 100 µM	-	-	-	+	+	-	-	-	-
W56 280 µM	-	-	-	-	-	+	+	-	-
F56 280 µM	-	-	-	-	-	-	-	+	+

c)

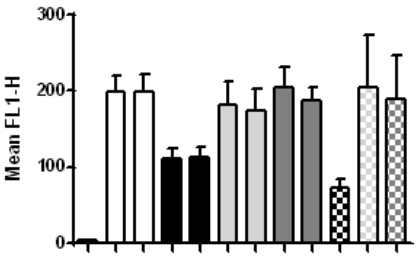

12G5	-	+	+	+	+	+	+	+	+	+	+
CXCL12	-	-	+	-	+	-	+	-	+	-	-
NSC23766 100 µM	-	-	-	+	+	-	-	-	-	-	-
AMD3100 5 µM	-	-	-	-	-	+	+	-	-	-	-
ATI2341 5 µM	-	-	-	-	-	-	-	+	+	-	-
post NSC23766	-	-	-	-	-	-	-	-	-	+	-
post AMD3100	-	-	-	-	-	-	-	-	-	-	+
post ATI2341	-	-	-	-	-	-	-	-	-	-	-

Figure 6

a)

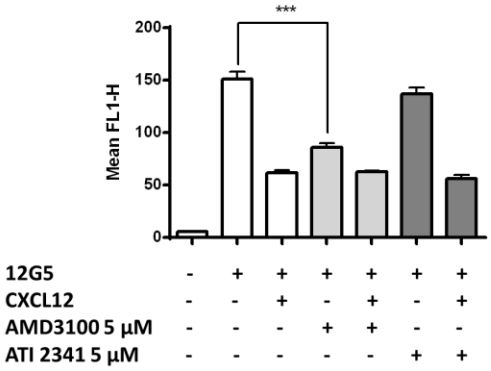

b)

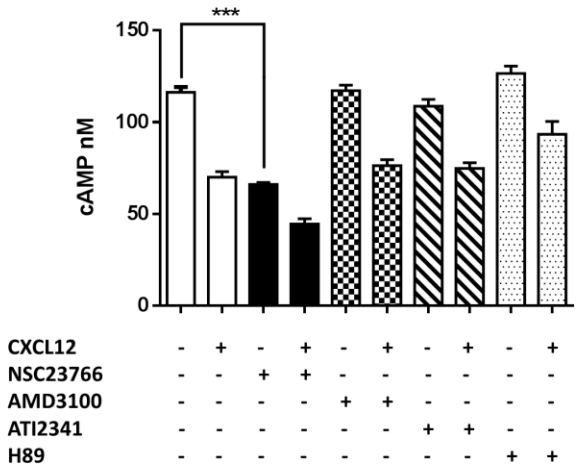

Figure 7

Highlights:

1) Rac1 is essential for CXCL12 induced migration in adherent cells as well as suspension cells
2) Rac1 activation is not needed for CCL3 induced cell migration
3) NSC23766, a Rac1 GEF inhibitor, acts as a ligand for CXCR4 and can initialise internalisation